to NO^+ have been noted previously in the crystal structures of complexes of the type $[Re(NO)X_4L]^-$ (X = Cl, L = pyridine; X = Br, L = EtOH, CH_3CN).[23] The technetium–bromide bond distances are unexceptional.

Acknowledgment. We thank the Biomedical Research Support-Shared Instrument Grant Program, Division of Research Resources, for funds to purchase the X-ray diffraction equipment (NIH Grant S10RR02243-01). This investigation was also supported (in part) by NIH Grant RR00317, Biotechnology Resources Branch, Division of Research Resources. We also gratefully acknowledge the financial support of NEN/DuPont, North Billerica, MA.

Registry No. $[^{99}Tc(CNCMe_3)_6]NO_3$, 101998-10-1; $[^{99}Tc(CNCMe_3)_6](PF_6)_2$, 102046-55-9; $[^{99}Tc(CNCMe_3)_6]PF_6$, 89172-45-2; $[^{99}Tc(CNCMe_3)_6]^{2+}$, 101998-11-2; $[Mn(CNCMe_3)_6]PF_6$, 38682-78-9; $[Mn(CNCMe_3)_6](PF_6)_2$, 23039-89-6; $^{99}Tc(NO)Br_2(CNCMe_3)_3$, 101998-12-3; $TBA[Tc(NO)Br_4]$, 90386-75-7.

Supplementary Material Available: Table S2, final thermal parameters, and Table S3, final hydrogen atom positional parameters (2 pages). Ordering information is given on any current masthead page. According to policy instituted Jan 1, 1986, Table S1, calculated and observed structure factors (6 pages), is being retained in the editorial office for a period of 1 year following the appearance of this work in print. Inquiries for copies of these materials should be directed to the Editor.

(23) (a) Ciani, G.; Guisto, D.; Manassero, M.; Sansoni, M. *J. Chem. Soc., Dalton Trans.* **1975**, 2156. (b) *Ibid.* **1978**, 798.

(24) The periodic group notation in parentheses is in accord with recent actions by IUPAC and ACS nomenclature committees. A and B notation is eliminated because of wide confusion. Groups IA and IIA become groups 1 and 2. The d-transition elements comprise groups 3 through 12, and the p-block elements comprise groups 13 through 18. (Note that the former Roman number designation is preserved in the last digit of the new numbering: e.g., III → 3 and 13.)

Contribution from the Department of Chemistry, Texas A&M University, College Station, Texas 77843

Redox Chemistry of Hydrogen Peroxide in Anhydrous Acetonitrile

Pablo Cofré and Donald T. Sawyer*

Received December 16, 1985

Under anhydrous conditions H_2O_2 is oxidized by a single-electron-transfer step to $HO_2^{\bullet}$, which (a) is further oxidized to O_2 by a second electron transfer or (b) disproportionates to H_2O_2 and O_2 (k_{MeCN}, 1×10^7 M^{-1} s^{-1}). The oxidation potential in dry acetonitrile (MeCN) for the primary process ($H_2O_2 + A^- \rightarrow HO_2^{\bullet} + HA + e^-$) ranges from +2.4 V vs. NHE to +1.8 V in the presence of p-$MePhSO_3^-$, +1.3 V with NH_3, and +1.0 V with picolinate anion. In MeCN, $HO_2^{\bullet}$ is reversibly reduced to HO_2^- at +0.64 V vs. NHE. These processes and the associated redox chemistry for H_2O_2 have been characterized at glassy-carbon (GC) electrodes by linear-sweep voltammetry and the rotated-ring–disk technique. Reduction of H_2O_2 at Pt (–0.4 V vs. NHE) or at GC (–1.5 V) yields H_2 and HO_2^-; the latter species is unstable ($HO_2^- + H_2O_2 \rightarrow O_2^{\bullet-} + H_2O + {}^{\bullet}OH$) but can be oxidized to $HO_2^{\bullet}$ at +0.64 V vs. NHE within the time frame of the ring–disk experiment (a few milliseconds).

The oxidation–reduction chemistry of dioxygen and of its reduced intermediates ($O_2^{\bullet-}$, $HO_2^{\bullet}$, and H_2O_2) in aprotic solvents has been a major interest of our group for the past 2 decades.[1,2] Hydrogen peroxide, which is a natural intermediate from aerobic metabolism,[3] can be generated from oxygen reduction or water oxidation and results from the proton-induced disproportionation of superoxide ion.[4]

$$2O_2^{\bullet-} + 2H^+ \rightarrow H_2O_2 + O_2 \quad (1)$$

The redox thermodynamics for hydrogen peroxide in aqueous media at pH 7 is summarized within the reduction manifold of Scheme I (with the standard state for O_2 unit activity).[5]

However, because of the water-like nature of hydrogen peroxide its redox properties are highly dependent upon the media and the solution acidity. The solvation energies for ionic intermediates have a primary effect on the redox potentials for H_2O_2. The enhanced solubility of O_2 in biomembranes and the presence of the reductive cofactors in the membrane prompts the conclusion that the generation of $O_2^{\bullet-}$ and H_2O_2 occurs in a nonaqueous matrix, which can be modeled by dipolar aprotic solvents such as acetonitrile.[6]

A previous study has discussed the electrochemical reduction of hydrogen peroxide in pyridine[7]

$$H_2O_2 + e^- \rightarrow {}^1/_2H_2 + HO_2^- \quad (2)$$

Scheme I

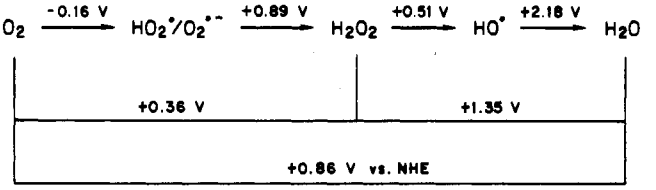

which is followed by a rapid chemical step to yield superoxide as the stable product (unique to pyridine because of its ability to trap ${}^{\bullet}OH$).[8]

$$H_2O_2 + HO_2^- \xrightarrow{py} O_2^{\bullet-} + H_2O + (1/n)[{}^{\bullet}py(OH)]_n \quad (3)$$

Beyond this the redox chemistry of H_2O_2 in aprotic media has been neglected. The present study is directed to the electron-transfer oxidation and reduction of H_2O_2 at glassy-carbon electrodes and to the generation and redox characterization of the intermediate product species, $HO_2^{\bullet}$ and HO_2^-, in acetonitrile (MeCN).

Experimental Section

Instrumentation. The rotated ring–disk electrode measurements were made with a Pine Instruments Co., Model PIR Rotator with either Pt–Pt- or GC–GC-ring–disk electrodes. The parameters of the electrodes were as follows: Pt–Pt electrode, r_1 = 0.382 cm, r_2 = 0.399 cm, r_3 = 0.422 cm, N = 0.178; GC–GC electrode, r_1 = 0.382 cm, r_2 = 0.416 cm, r_3 = 0.556 cm, N = 0.418. Potential control was provided by a Pine Instruments Co., Model RDE 3 dual potentiostat. The sample solutions and electrode assembly (including a Pt auxiliary electrode in a separate tube with a medium-porosity fritted-glass disk at the end and a Ag/AgCl reference electrode in a Luggin capillary) were contained in a 150-mL

(1) Wilshire, J.; Sawyer, D. T. *Acc. Chem. Res.* **1979**, *12*, 105–110.
(2) Sawyer, D. T.; Valentine, J. S. *Acc. Chem. Res.* **1981**, *14*, 393–400.
(3) Hemmerich, P.; Wessiak, A. In *Biochemical and Clinical Aspects of Oxygen*; Caughey, W. S., Ed.; Academic: New York, 1979; pp 491–511.
(4) Chin, D. H.; Chiericato, G., Jr.; Nanni, E. J., Jr.; Sawyer, D. T. *J. Am. Chem. Soc.* **1982**, *104*, 1296–1299.
(5) Sawyer, D. T.; Roberts, J. L., Jr.; Tsuchiya, T.; Srivatsa, G. S. In *Oxygen Radicals in Chemistry and Biology*; Bors, W., Saran, M., Tait, D., Eds.; Walter de Gruyter: Berlin, New York, 1984; pp 25–34.
(6) Sawyer, D. T.; Roberts, J. L., Jr.; Calderwood, T. S.; Sugimoto, H.; McDowell, M. S. *Philos. Trans. R. Soc. London, B* **1985**, 311, 483–503.
(7) Morrison, M. M.; Roberts, J. L., Jr.; Sawyer, D. T. *Inorg. Chem.* **1979**, *18*, 1971–1973.
(8) Roberts, J. L., Jr.; Morrison, M. M.; Sawyer, D. T. *J. Am. Chem. Soc.* **1978**, *100*, 329–330.

0020-1669/86/1325-2089$01.50/0

beaker with a Leeds and Northrup plastic cell top.

The ring currents and disk currents vs. disk potential in the collection-efficiency experiments were recorded simultaneously on two Houston Model 2000 X-Y recorders. The linear-sweep voltammetric experiments were accomplished with the same instruments and electrodes.

Reagents and Solvents. Acetonitrile (MeCN) was supplied from Burdick and Jackson ("distilled in glass grade") and had a water content of 0.007%. All solutions contained 0.1 M tetraethylammonium perchlorate (TEAP) (reagent grade, G. F. Smith Chemical Co.) as supporting electrolyte. This salt was vacuum-dried prior to addition to the MeCN solvent.

The starting material for the preparation of anhydrous H_2O_2 was a certified 50% hydrogen peroxide solution (stabilized) from Fisher Scientific Allied Co. Fifteen milliliters of this solution was placed in a 50-mL round-bottom flask for vacuum distillation. All of the glassware used had been thoroughly cleaned by soaking in concentrated nitric acid overnight, followed by soaking in a 0.1 M EDTA solution. The H_2O_2 solution was frozen with liquid nitrogen before the system was evacuated. The vacuum distillation was carried out at room temperature until the volume of H_2O_2 left in the flask was reduced to one-third. Samples of the resulting anhydrous H_2O_2 were weighed and titrated with standardized potassium permanganate solution. The assay for H_2O_2 was 96.3%. A 0.1 M H_2O_2 stock solution in MeCN was prepared immediately and stored in a refrigerator. Titration of this stock solution after 10 days confirmed that its H_2O_2 content was unchanged.

Tetramethylammonium *p*-toluenesulfonate (TMAPTS) was prepared by reaction of tetramethylammonium hydroxide pentahydrate (TMAOH) from Southwestern Analytical Chemicals Inc., and *p*-toluenesulfonic acid from MCB Manufacturing Chemists Inc. Tetramethylammonium picolinate (TMAPIC) was prepared by neutralization of picolinic acid 99% from Aldrich Chemical Co., Inc., with TMAOH. After the acids were neutralized with TMAOH in aqueous solutions, the solutions were freed of water in a rotary evaporator. The resulting solids were recrystallized twice: the TMAPTS from methanol and TMAPIC from MeCN. The final products were vacuum-dried for 2 days prior to use. Direct acid-base titration of TMAPIC and indirect (after ion exchange with Dowex 50W, 100-200 mesh resin) of TMAPIC gave assays of 99% and 100% purity, respectively. Stock solutions of both salts (0.05 M) were prepared by direct weighing. A stock solution of ammonia (99.99%, Matheson Gas Products) in MeCN was prepared by bubbling into MeCN, and was standardized by an acid-base titration. The solubility of NH_3 in MeCN was found to be 1.03 M (1 atm).

Results

Oxidation of H_2O at a GC Electrode. Figure 1A illustrates cyclic voltammograms for anhydrous H_2O_2 in dry MeCN. The anodic peak current increases linearly with the H_2O_2 concentration and is proportional to the square root of the scan rate for a given H_2O_2 concentration. After the peak potential is passed during the voltage scan, there is not a smooth decay of the current; a current plateau occurs, which indicates the presence of secondary electrode processes before the onset of the solvent-oxidation front. The H_2O_2-oxidation electrode reaction partially overlaps with that for the oxidation of trace water. The latter process deactivates the GC electrode surface, but reproducible results are obtained by resurfacing the electrode prior to each scan.

The voltammetric oxidation of H_2O_2 at a rotated disk electrode yields a peaked anodic wave with a half-wave potential ($E_{1/2}$) of +2.1 V vs. SCE The maximum current (I) for H_2O_2 oxidation at the rotated disk electrode is directly proportional to the concentration of H_2O_2, and is consistent with a first-order diffusion-controlled process.

In the presence of base the oxidation of H_2O_2 is facilitated, which results in a shift in the anodic half-wave potential to less positive potentials; the shift is proportional to the pK_a values for the base (Table I). The trace-water oxidation wave also is shifted to less positive potentials in the presence of these bases. The H_2O_2 oxidation wave in the presence of base preserves its plateau until the electrode potential increases to the onset of the water oxidation wave. At that point the current begins to decrease as the electrode becomes passivated. If the electrode potential is kept below the trace-water oxidation potential, the electrode activity is preserved from one scan to the next.

Characterization of Oxidation Products. In a rotated ring-disk electrode experiment where the disk is controlled at +2.6 V vs. SCE for the oxidation of H_2O_2 and the ring electrode is controlled at −1.4 V vs. SCE for the reduction of the oxidation products from

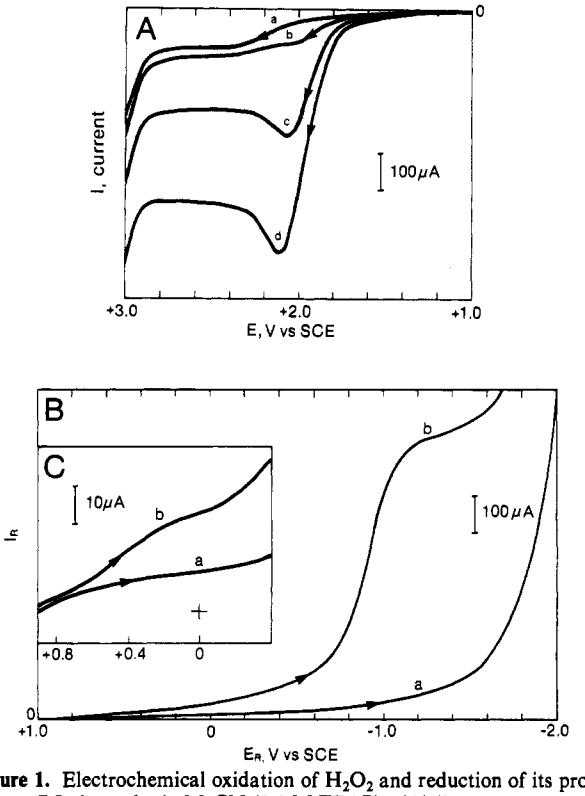

Figure 1. Electrochemical oxidation of H_2O_2 and reduction of its products at GC electrodes in MeCN (0.1 M TEAP): (A) linear-sweep anodic voltammograms for (a) 0, (b) 0.3, (c) 1.7, and (d) 3.3 mM H_2O_2 (scan rate, 2 V min^{-1}; electrode area, 0.46 cm^2); (B) rotated ring electrode cathodic voltammogram (scan rate, 10 mV s^{-1}) of the product from the oxidation of 4 mM H_2O_2 at the rotated disk electrode (rotation rate, 1600 rpm) for (a) E_D disconnected, and (b) E_D = +2.6 V vs. SCE; (C) rotated ring electrode cathodic voltammogram (scan rate, 10 mV s^{-1}) of the products from the oxidation of 1 mM H_2O_2 at the rotated disk electrode (rotation rate, 4900 rpm) for (a) E_D disconnected and (b) E_D = +2.6 V vs. SCE.

Table I. Effect of 10 mM Base on the Oxidation Potential ($E_{1/2}$) of 4 mM H_2O_2 in MeCN

	base[a]			
	ClO_4^-	$MePhSO_3^-$	NH_3	PA^-
pK_a[b]	−8.3	−3.3	+6.4	+9.1
$E_{1/2}$,[c] V vs. SCE	+2.1	+1.6	+1.1	+0.8

[a] Key: $MePhSO_3^-$, *p*-toluenesulfonate; PA^-, picolinate. [b] pK_a values determined by linear-sweep voltammetry (see ref 11). [c] $E_{1/2}$ values from anodic voltammograms at a glassy-carbon rotated disk electrode (1600 rpm); scan rate = 0.01 V s^{-1}.

H_2O_2, the observed collection efficiency ($N = I_R/I_D$) is 0.384. This is slightly less than the theoretical value of 0.418. The products from H_2O_2 oxidation at the GC disk electrode (E_D = +2.6 V vs. SCE) can be characterized at the ring by scanning its potential from +1.0 to −2.0 V vs. SCE. Figure 1B illustrates the reduction of the products from the oxidation of 4 mM H_2O_2. The first and second of the three reduction waves ($E_{1/2}$ = +0.4 V vs. SCE) are better resolved at a lower concentration of H_2O_2 and a higher rotation rate (Figure 1C). The second ($E_{1/2}$ = −0.2 V vs. SCE) and third ($E_{1/2}$ = −0.95 V vs. SCE) reductions are charcteristic of O_2 reduction in the presence of protons[4] for this solvent and electrode material. Introduction of oxygen into the cell results in a proportionate increase for the currents of these waves.

The potential for the first reduction wave ($E_{1/2}$ = +0.4 V vs. SCE) is consistent with that for $HO_2^{\bullet}$.[9] If the collection efficiencies (N_{exptl}) are determined with the ring-electrode potential at a more positive value (E_R = +0.1 V vs. SCE), a smooth decay in the N_{exptl} values is obtained as the bulk H_2O_2 concentration

(9) Cofrē, P.; Sawyer, D. T. *Anal. Chem.*, in press.

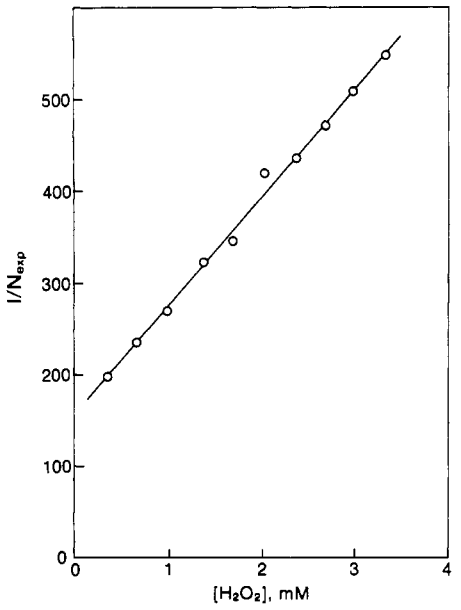

Figure 2. Experimental collection efficiencies (N_{exptl}) at the rotated ring electrode as a function of H_2O_2 concentration for the product from the oxidation of H_2O_2 at the rotated disk electrode. Control conditions for GC ring–disk electrode: rotation rate, 4900 rpm; E_D, +2.6 V vs. SCE; E_R, +0.1 V vs. SCE.

is increased. A plot of $1/N_{exptl}$ against H_2O_2 concentration yields a straight line as shown in Figure 2. The $HO_2^{\bullet}$/disproportionation reaction rate constant (k) can be calculated from these data if (a) the oxidation of H_2O_2 is a diffusion-controlled process (indicated by the scan-rate dependence of voltammetric peak current) and (b) the only decay path for $HO_2^{\bullet}$ is its disproportionation in solution while traversing from the disk electrode to the ring electrode. The disproportionation of $HO_2^{\bullet}$ follows a simple second-order rate law

$$1/[HO_2^{\bullet}]_t - 1/[HO_2^{\bullet}]_0 = kt \qquad (4)$$

where $[HO_2^{\bullet}]_t$ is the concentration at the inner edge of the ring electrode after a reaction time "t" and $[HO_2^{\bullet}]_0$ is the surface concentration at the disk (or zero-time concentration). For a diffusion-controlled process, the latter (at the limiting current condition for the oxidation of H_2O_2) is equal to the bulk H_2O_2 concentration.

The experimental collection efficiencies N_{exptl}, when compared to the theoretical N, make it possible to relate the two $HO_2^{\bullet}$ concentrations ($[HO_2^{\bullet}]_t$ and $[HO_2^{\bullet}]_0$):

$$[HO_2^{\bullet}]_t = (N_{exptl}/N)[HO_2^{\bullet}]_0$$

Substitution in eq 4 gives

$$1/N_{exptl} = 1/N + (kt/N)[H_2O_2]$$

From the slope of a plot of $1/N_{exptl}$ vs. $[H_2O_2]$ the value for the second-order rate constant (k) has an approximate value of $(1.0 \pm 0.5) \times 10^7$ M^{-1} s^{-1}. This result is based on a value of 0.418 for N and an estimate of 27 ms for the time to traverse the gap between the ring electrode and the disk electrode.[10]

Reduction of H_2O_2. The reduction of H_2O_2 at GC and Pt rotated disk electrodes yields well-defined voltammetric waves (Figure 3A). The reduction potential at Pt is much less negative than at GC, which is consistent with proton reduction. The products from the reduction of H_2O_2 on a GC electrode (E_D = −2.0 V vs. SCE) can be detected and characterized at the ring electrode by scanning its potential from −0.5 to +3.0 V vs. SCE (Figure 3B). Curve a illustrates the oxidation of H_2O_2 at the ring electrode when the disk electrode is disconnected. With the disk electrode at a potential that reduces H_2O_2, curve b illustrates that the ring electrodes yields a new oxidation wave at $E_{1/2}$ = +0.4

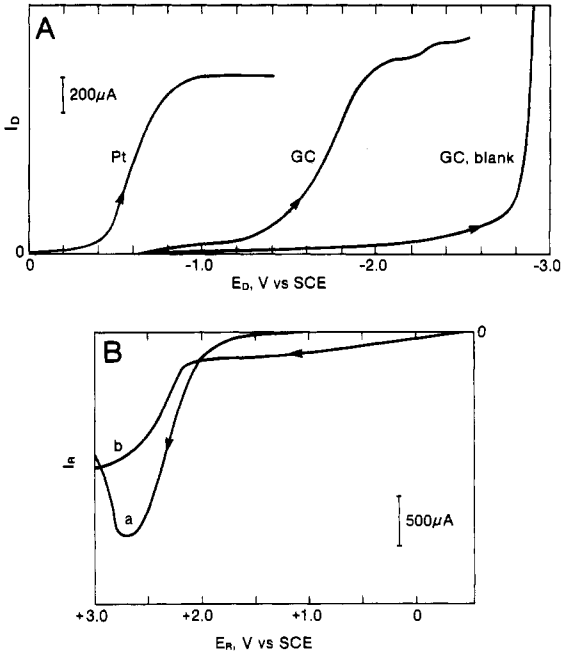

Figure 3. Electrochemical reduction of H_2O_2 in MeCN (0.1 M TEAP) at rotated GC- and Pt-disk electrodes (rotation rate, 1600 rpm): (A) 2 mM H_2O_2, scan rate = 10 mV s^{-1}; (B) oxidation of products at GC ring electrode (scan rate, 10 mV s^{-1}) from the reduction of 1 mM H_2O_2 at GC disk electrode (rotation rate, 1600 rpm) for (a) E_D disconnected and (b) E_D = −2.0 V vs. SCE.

V vs. SCE and a lower current for H_2O_2 oxidation (a decrease in concentration). The first wave appears to be due to the oxidation at the ring electrode of the HO_2^- that is generated from the reduction of H_2O_2 on the disk electrode.

Discussion and Conclusions

The results of Figure 1 and the associated electrochemical studies are consistent with an overall oxidation of H_2O_2 to O_2.

$$H_2O_2 \rightarrow O_2 + 2H^+ + 2e^- \qquad (5)$$

Although the process is diffusion controlled and chemically reversible, the absence of a reverse peak confirms that the oxidation is electrochemically irreversible and not a simple concerted two-electron step. On the basis that (a) the collection efficiency (N_{exptl}) at −1.4 V vs. SCE for the products of H_2O_2 oxidation is less than that for a simple electron-transfer process, (b) a product species from H_2O_2 oxidation other than O_2 is reduced at +0.4 V vs. SCE (Figure 1C), and (c) the presence of base shifts the oxidation potential to much less positive values (Table I), we propose that the primary step for the oxidation of H_2O_2 is a single-electron transfer.

$$H_2O_2 \rightleftharpoons H_2O_2^{\bullet+} + e^- \quad E_{1/2} = +2.1 \text{ V vs. SCE}$$
$$\downarrow$$
$$HO_2^{\bullet} + H^+ \qquad (6)$$

The data of Table I confirm that the presence of bases in the electrolysis medium shifts the potential for H_2O_2 oxidation to a degree that is directly proportional to the pK_a of the base. Hence, a reasonable oxidation path involves direct formation of $HO_2^{\bullet}$ and protonated base (HA)

$$H_2O_2 + A^- \rightarrow HA + HO_2^{\bullet} + e^- \qquad (7)$$
$$(E_{1/2})_{PA^-} = +0.8 \text{ V vs. SCE}$$

where A^- represents picolinate anion (PA^-) with a pK_a value of 9.1 in MeCN.[11]

The perhydroxyl radical ($HO_2^{\bullet}$) that results from the primary step of H_2O_2 oxidation (eq 6 or 7) is more easily oxidized than

(10) Bruckenstein, S.; Napp, D. T. *J. Am. Chem. Soc.* **1968**, *90*, 6303–6309.

(11) Barrette, W. C., Jr.; Johnson, H. W., Jr.; Sawyer, D. T. *Anal. Chem.* **1984**, *56*, 1890–1898.

H_2O_2. Such an oxidation is the reverse of the primary step for the reduction of O_2 in the presence of Brønsted acids,[9] and its potential is dependent upon the basicity of the medium. If the picolinate anion is assumed to provide a proton "sink" comparable to dimethylformamide (a neutral pH), then a reasonable estimate for the potential for $HO_2^{\bullet}$ oxidation is the value of O_2 reduction in such protonated media.[4]

$$HO_2^{\bullet} + A^- \rightarrow O_2 + HA + e^- \qquad (E_{1/2})_{PAH/PA^-} = -0.2 \text{ V vs. SCE} \tag{8}$$

In the absence of bases the initial product from the oxidation of H_2O_2 (eq 6), $H_2O_2^{\bullet+}$, escapes from the disk-electrode surface before it dissociates. The data for Figure 1C indicate that the resulting $HO_2^{\bullet}$ species is reduced at the ring electrode.

$$HO_2^{\bullet} + H^+ + e^- \rightarrow H_2O_2 \qquad E_{1/2} = +0.40 \text{ V vs. SCE} \tag{9}$$

The results that are illustrated by Figure 2 indicate that the $HO_2^{\bullet}$ species is subject to rapid disproportionation

$$HO_2^{\bullet} + HO_2^{\bullet} \rightarrow H_2O_2 + O_2 \qquad k_{bi} = 1.0 \times 10^7 \text{ M}^{-1} \text{ s}^{-1} \tag{10}$$

which causes its collection effeciency (N_{expt}) to decrease with larger H_2O_2 concentrations and slower rates of rotation. The value of the second-order rate constant (k_{bi}) in MeCN solution is based on several assumptions for the ring–disk experiment, but appears reasonable in relation to values of 8.6×10^5 M^{-1} s^{-1} in aqueous solutions[12] and $>1 \times 10^7$ M^{-1} s^{-1} in dimethylformamide.[4] A previous discussion[13] outlines the experimental results in support of a disproportionation mechanism for $HO_2^{\bullet}$ that does not involve O–O bond cleavage or formation of $^1O_2$, but homolytic cleavage of an O–H bond within a dimer.

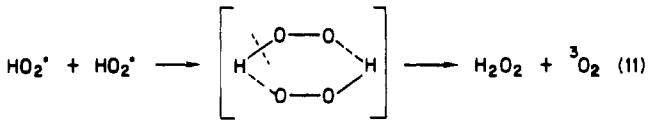

When $HO_2^{\bullet}$ is produced by electron-transfer reduction of O_2 in the presence of protons,[9] it is specifically adsorbed to the electrode surface (probably as a dimer) and catalytically disproportionated. In contrast, the electron-transfer oxidation of H_2O_2 at a glassy-carbon (GC) surface does not result in such specific adsorption; $HO_2^{\bullet}$ is reduced at the rotated ring electrode ($E_{1/2}$ = +0.4 V vs. SCE; Figure 1C). The apparent reason for this different behavior is modification of the GC surface that results from cooxidation of residual H_2O in the solvent ($H_2O \rightarrow {}^{\bullet}OH + H^+ + e^-$), which blocks the specific adsorption sites for $HO_2^{\bullet}$.

In a recent study[9] the reduction of $HO_2^{\bullet}$ (formed from $O_2^{\bullet-}$ plus protons) in the presence of 4 mmol of $HClO_4$ (0.1 M aqueous solution) has been observed at a rotated GC-disk electrode.

$$HO_2^{\bullet} + H_3O^+ + e^- \rightarrow H_2O_2\,(H_2O) \qquad E_{1/2} = +0.2 \text{ V vs. SCE} \tag{12}$$

The conditions for the oxidation of H_2O_2 (Figure 1) are much more anhydrous. Hence, reduction of the oxidation products ($HO_2^{\bullet} + H^+$) occurs at a more positive potential (in MeCN, water acts as a base).

$$HO_2^{\bullet} + H^+ + e^- \rightarrow H_2O_2 \qquad E_{1/2} = +0.4 \text{ V vs. SCE} \tag{13}$$

Because the electrochemical reduction of H_2O_2 involves proton reduction, the potential for the process is strongly dependent on electrode material (Figure 3).[11]

$$H_2O_2 + e^- \rightarrow {}^1/_2H_2 + HO_2^- \qquad (E_{1/2})_{GC} = -1.7 \text{ V vs. SCE} \quad (E_{1/2})_{Pt} = -0.6 \text{ V vs. SCE} \tag{14}$$

The less negative potential at Pt is the consequence of the stabilization of atomic hydrogen [H•(Pt)]. The previous investigation of H_2O_2 reduction failed to detect the HO_2^- species because of its instability.[7]

$$HO_2^- + H_2O_2 \rightarrow O_2^{\bullet-} + H_2O + {}^{\bullet}OH \tag{15}$$

Thus, in pyridine the reduction of H_2O_2 via cyclic voltammetry yields $O_2^{\bullet-}$ as the only detectable oxidizable product. However, at a rotated GC-disk electrode, reduction of H_2O_2 yields an intermediate species that is oxidized at the GC-ring electrode (Figure 3B).

$$HO_2^- \rightarrow HO_2^{\bullet} + e^- \qquad E_{1/2} = +0.4 \text{ V vs. SCE} \tag{16}$$

The goal of the present study has been to ascertain the redox thermodynamics for H_2O_2 within anhydrous acetonitrile that contains picolinate anion. The latter is assumed to be a reasonable model matrix for proteinaceous biomembranes. For such a medium the preceding results can be cast into a redox manifold:

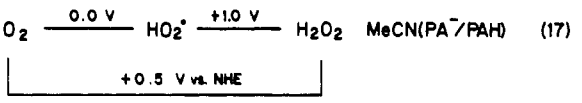

When the model matrix contains excess protons, a reasonable set of half-reaction potentials can be estimated from the present electrochemical measurements.

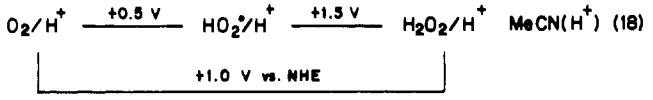

These potentials are referenced to the normal hydrogen electrode (NHE, +0.246 V vs. SCE). Although the assumption of a negligible junction potential between an aqueous saturated calomel electrode and the acetonitrile matrix is arbitrary, analysis of this problem in a recent electrochemical evaluation of pK_a constants[11] indicates that the error in the measured potentials is less than ±0.03 V. Furthermore, because all of the measured redox potentials for dioxygen species have used the same reference electrode, their relative values are independent of the junction potential.

Comparison of the neutral aqueous H_2O_2 redox potentials (Scheme I) with those for the neutral model membrane matrix (eq 17) indicates a positive shift of +0.1 to +0.2 V for each couple in the nonaqueous system. The instability of $HO_2^{\bullet}$ toward disproportionation in each matrix can be calculated from the redox manifolds of Scheme I and eq 17, respectively [$\log K = (E_2 - E_1)/0.05915$].

$$2HO_2^{\bullet} \rightarrow H_2O_2 + O_2 \qquad K_{H_2O(pH\,7)} = 10^{18} \quad K_{MeCN(PA^-)} = 10^{17} \tag{19}$$

These data indicate that the matrix only has a slight effect.

Acknowledgment. This work was supported by the National Institutes of Health under Grant No. GM-36289 and the National Science Foundation under Grant No. CHE 82-12299. We are especially grateful to Dean Rafael Gana of the Catholic University, Santiago, Chile, for the award of a sabbatical leave to Prof. Pablo Cofrê.

Registry No. H_2O_2, 7722-84-1; ClO_4^-, 14797-73-0; $MePhSO_3^-$, 16722-51-3; PA^-, 98-98-6; NH_3, 7664-41-7; $HO_2^{\bullet}$, 3170-83-0; HO_2^-, 14691-59-9; H_2, 1333-74-0; C, 7440-44-0; Pt, 7440-06-4; O_2, 7782-44-7.

(12) Bielski, B. H. J. *Photochem. Photobiol.* **1978**, *28*, 645–649.
(13) Roberts, J. L., Jr.; Sawyer, D. T. *Isr. J. Chem.* **1983**, *23*, 430–438.